УДК 539.1.07.3

INFLUENCE OF INHOMOGENEITIES IN SCINTILLATING FIBRE ELECTROMAGNETIC CALORIMETER ON ITS ENERGY RESOLUTION

P.Štavina[1], *S.Tokár*[1], *J.A.Budagov*[2], *I.Chirikov-Zorin*[2], *D.Pantea*[3]

The specific aspects related to the discrete structure of the scintillating fibre electromagnetic calorimeter are investigated by means of Monte-Carlo simulation. It is shown that the structure inhomogeneity leads to an additional contribution to the systematic term in the energy resolution parametrization formula which weakly depends on energy and to the distortion of the Gaussian form of response distribution. The investigation was carried out for small tilt angles and for the absorber-to-fibre ratio 4:1.

The investigation has been performed at the Laboratory of Nuclear Problems, JINR.

Влияние неоднородностей в сцинтилляционном волоконном электромагнитном калориметре на энергетическое разрешение

Ставина П. и др.

Методом Монте-Карло исследованы специфические аспекты, связанные с дискретной структурой сцинтилляционного волоконного электромагнитного калориметра. Показано, что неоднородность структуры ведет к дополнительному вкладу в систематический член в формуле параметризации энергетического разрешения, слабо зависящий от энергии, и искажает гауссову форму распределения отклика. Исследования были выполнены для небольших углов наклона и отношения поглотитель—волокно 4:1.

Работа выполнена в Лаборатории ядерных проблем ОИЯИ.

Introduction

Scintillating fibre calorimeters (SciFi) belong to the class of heterogeneous calorimeters. In addition to the common characteristics that SciFi calorimeters share with other heterogeneous calorimeters (e.g., the sandwich ones), they have some specific features stemming from peculiarities of the SciFi calorimeter structure.

The SciFi calorimeters are usually operated in such a way that the directions of particles to be detected are nearly parallel to the direction of the fibres. Depending on the impact point position on the calorimeter surface the shower development will start under

[1]Dept. of Nuclear Physics, Comenius University, Mlynská Dolina F1, SK-84215 Bratislava, Slovak Republic.
[2]Joint Institute for Nuclear Research, 141980 Dubna, Moscow Region, Russia.
[3]Institute of Atomic Physics, P.O.Box MG-6 Bucharest, Romania.

different initial conditions. Hence, the mean calorimeter response, and thereby the energy resolution, is expected to fluctuate depending on the place of incidence (fibre or absorber). By calorimeter response we understand the energy released in the active material (scintillating fibres). It was shown [1,2] that the energy resolution of the electromagnetic SciFi calorimeter is better when only particles (electrons) entering lead were taken into account. A similar calorimeter dependence on the incident particle impact point was also observed at the liquid Argon electromagnetic «accordion-like» calorimeter [3]. This suggests separate investigation of two situations:

- The impact point position is fixed and then the calorimeter response is Gaussian distributed. Its mean value and standard deviation are different depending on the place of incidence, i.e., either fibre or absorber.
- No distinction on the impact point position is made and the calorimeter response is distributed as a sum of Gaussians with different mean values and standard deviations.

Moreover, due to the SciFi calorimeter structure (fibres whose diameter is usually 1 mm or less and which are imbedded in a matrix of the absorber) the energy flow of delta electrons through the contact surface between the active and passive media could play an important role.

The above-mentioned circumstances should be taken into account in the Monte Carlo (MC) simulations and the interpretation of the test beam SciFi calorimeter energy resolution measurements.

In the present paper we have investigated a possible effect of the discrete structure of the SciFi calorimeter on its energy resolution using the MC method. The manifestation of the calorimeter discrete structure should be seen more clearly at high passive-to-active material volume ratios and small tilt angles. Most of the simulations were done for the tilt angle 3° and the volume ratio approximately 4:1, assuming a mixture of lead and glue as the passive material. The 4:1 ratio was chosen because it was the highest ratio used in practice [4]. In our study we concentrated on the influence of the calorimeter discrete structure on the energy resolution constant term and on the response function shape. It is very important to understand the nature of the constant term as fluctuations connected with this term govern the energy resolution at high energies, where the role of sampling fluctuations is diminished.

The energy resolution is usually parametrized by the formula:

$$\frac{\sigma}{E} = \frac{a}{\sqrt{E}} \oplus b. \tag{1}$$

The coefficient $a = \sqrt{a_1^2 + a_2^2}$ has a statistical nature and represents the combined effect of sampling (a_1) and photostatistics (a_2) fluctuations. The coefficient b characterises the systematic effects connected with structure inhomogeneity, energy leakage [5], light attenuation in fibres [6,7], calibration procedure and nonuniformity of active medium [8], etc. The operation $\oplus$ means that the stochastic ($a/\sqrt{E}$) and the systematic (b) terms are summed quadratically. Sometimes in the literature [4] these terms are added linearly. In our treatment the quadratic addition of the stochastic and systematic terms appears naturally and has a neat physical interpretation. Note that the photostatistics fluctuations are not taken into account ($a_2 = 0$) in this paper.

Following the arguments presented above, the average response of the SciFi calorimeter can depend on the incident point. For clarity, we defined the global and local energy resolutions. The former corresponds to the calorimeter response distribution obtained for a beam where incident points are scattered over a large (compared to fibre-to-fibre distance) area of the calorimeter surface (global response distribution). The latter corresponds to the response distribution for a fixed incident point (local response distribution).

The present paper is organised as follows. In section 2, we analyse the relation between the shape of the global and local responses of the SciFi calorimeter. In section 3, we describe the Monte Carlo (MC) method employed for studying the SciFi calorimeter inhomogeneities and present the results of this study. Conclusions are given in section 4.

2. Shape of Global Response Distribution

We can understand the role which the SciFi calorimeter discrete structure plays in its energy resolution from the study of the relation between the global and local responses of the calorimeter, i.e., what happens with the calorimeter response when the beam spot diameter on the calorimeter front face becomes large (in the sense mentioned above) and when this diameter is shrinking to zero.

If one uses a wide-spot beam for the study of the SciFi calorimeter energy resolution, the result is a global response distribution. This distribution is built up from the responses for different impact points scattered over the calorimeter surface. Each of the incident points can be characterised by its own response distribution (local response distribution) which is a Gaussian with the mean value $\bar{E}_i$, the average local response, and the corresponding standard deviation σ_i (i is the index of the impact point).

One can express the global response distribution, w_{gl}, for N impact points in the following form:

$$w_{gl}(E) = \frac{1}{N} \sum_{i=1}^{N} \frac{1}{\sqrt{2\pi}\sigma_i} \exp\left(-\frac{(E - \bar{E}_i)^2}{2\sigma_i^2} \right). \tag{2}$$

For this distribution we can calculate its global mean value ($\bar{E}$) and variance (σ^2):

$$\bar{E} = \frac{1}{N} \sum_{i=1}^{N} \bar{E}_i, \tag{3}$$

$$\sigma^2 = \frac{1}{N} \sum_{i=1}^{N} \sigma_i^2 + \frac{1}{N} \sum_{i=1}^{N} \bar{E}_i^2 - \left(\frac{1}{N} \sum_{i=1}^{N} \bar{E}_i \right)^2. \tag{4}$$

Note that the variance of this distribution consists of two components:

$$\sigma^2 = \sigma_0^2 + \sigma_{non}^2 \tag{5}$$

with

$$\sigma_0^2 = \frac{1}{N}\sum_{i=1}^{N}\sigma_i^2$$

and

$$\sigma_{\text{non}}^2 = \frac{1}{N}\sum_{i=1}^{N}\bar{E}_i^2 - \left(\frac{1}{N}\sum_{i=1}^{N}\bar{E}_i\right)^2. \tag{6}$$

The value of the average local response $\bar{E}_i$ depends on the position of the impact point on the calorimeter surface. The standard deviation σ_{non} characterises the fluctuations of $\bar{E}_i$ over the calorimeter surface due to inhomogeneity of the SciFi calorimeter. It was found [9] that at first stage of shower development (first 2—3 X_0) the secondary particles are produced very collimated in the direction of the shower parent particle. For a small tilt angle almost all of these particles are contained in lead or in fibres depending on the incident point position, and $\bar{E}_i$, the mean energy released in the active medium, is accordingly lower or higher.

Looking at the structure of the two terms present in the expression of global variance σ^2 given by (4), one can notice that the sampling fluctuations are contained in σ_0 through the standard deviations related to each impact point position. The second term, σ_{non}, characterises only the spread of released mean energy values, which is a systematic effect due to calorimeter inhomogeneity. This effect is expected to be independent or to show weak dependence on the incident energy.

One must notice that the quadratic addition of the two terms in (4) stochastic (σ_0) and systematic (σ_{non}), appeared in our treatment in a natural way. From the above, it follows that the global response distribution is wider than the local one. In addition, one can expect that the former should have a non-Gaussian shape with a tail towards the high energies. The reasons for such behaviour stem from the Poissonic nature of the process of energy deposition in active medium. Taking into account the Poissonic nature of the process one can express σ_i as

$$\sigma_i = \text{const}\sqrt{\bar{E}_i} \approx \sigma_a\left(1 + \Delta\frac{\bar{E}_i - \bar{E}}{\sigma_a}\right), \tag{7}$$

where $\sigma_a = \text{const}\sqrt{\bar{E}}$ and one could expect that $\sigma_a = \sigma_0$, $\bar{E}$ is defined as before and $\Delta = \text{const}/(2\sqrt{\bar{E}})$ is an asymmetry parameter.

The increase of σ_i with the mean deposited energy $\bar{E}_i$ brings about a right tail in the global response distribution $w_{\text{gl}}(E)$. The from of this distribution could be expressed analytically using expressions (2) and (7) and provided that the average local response $\bar{E}_i$ has Gaussian distribution (see appendix A).

In the next section it is shown that the simulation data support this behaviour.

3. Results of SciFi Response Simulation

The effect of the calorimeter inhomogeneity was investigated by Monte-Carlo simulation. The simulation of the SciFi calorimeter was made with a code based on the GEANT package [10]. The structure of the simulated calorimeter, the definition of axes, the tilt angle, azimuthal angle, and the size of a calorimeter module are shown in Fig.1. The scintillating fibres were placed in a hexagonal matrix with each fibre equidistant to its neighbours. The absorber-to-fibre volume ratio used in the calculations was 4.17:1 assuming a mixture of lead (≈ 99%) and glue (≈ 1%) as an absorber. To investigate the effects originating in the discrete structure of the SciFi calorimeter we assumed that no other systematic effects are present, i.e., the fibres are ideal (no fibre-to-fibre response fluctuations and no light attenuation) with the same diameters and the same fibre-to-fibre distances. The energy leakage is negligible for this calorimeter (~ 56 radiation lengths).

To take into account a possible effect of the delta electrons (see introduction) the energy cut-offs [10] for all types of particles were set to 10 keV and above this threshold the delta electrons were generated explicitly. It was found that the explicit treatment of delta electrons leads to higher values of the sampling fraction which is in better agreement with experimental data.

In order to investigate in detail the inhomogeneity effect, the scanning of the local calorimeter response was done from the central fibre to its neighbour as is shown by the dotted line in Fig.2. The dependence of the SciFi calorimeter response mean value on the impact point was investigated in this case. To demonstrate the effect we simulated the calorimeter response at the tilt angle 1°, where significant oscillations could be expected. The results of the simulations are depicted in Fig.3, where these oscillations are visible. This effect was seen experimentally by the SPACAL collaboration [2]. The period of these oscillations is approximately 3.8 mm as expected (see Fig.2). A shift of the maximum position by about 0.5 mm from the true position of the fibre centre is due to the tilt angle. An additional local maximum at around 2.4 mm from the central fibre is caused by the closest fibres neighbouring columns. Note also the same 0.5 mm shift as before. The dependence of the average response on the azimuthal angle is weak [7].

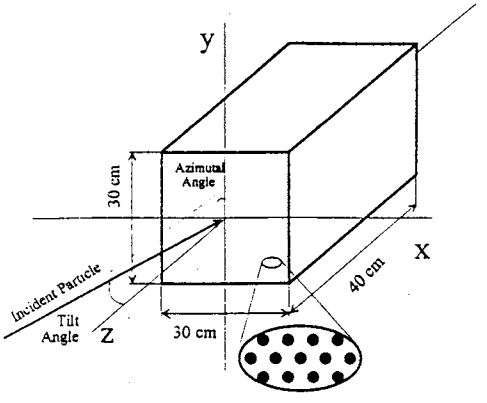

Fig.1. Structure of the simulated scintillating fibre calorimeter

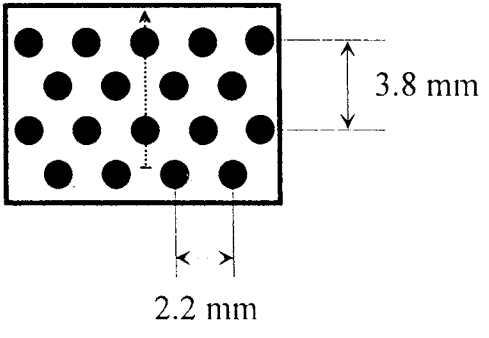

Fig.2. Direction of the local calorimeter response scan

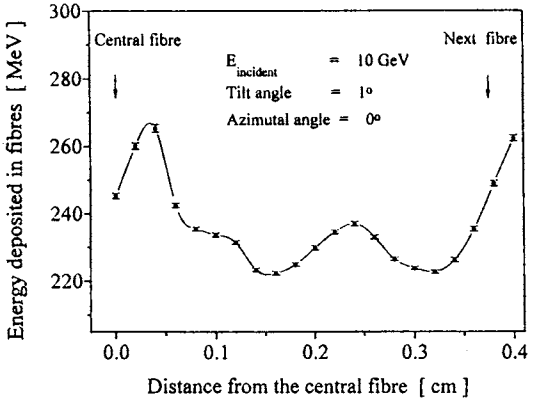

Fig.3. Mean deposited energy in the active material (fibres) as a function of the impact point

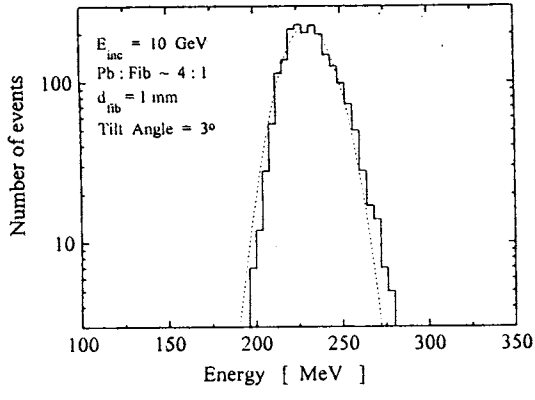

Fig.4. Simulated response function of the scintillating fibre calorimeter for the 10 GeV incident particle at the tilt angle 3°

In Fig.4 a typical response function is plotted for 10 GeV electrons and a wide (1×1 cm^2) beam. From this figure one can see that the response distribution has a non-Gaussian shape with the right tail enhanced, which is in good agreement with (A.2) and clearly manifests the response nonuniformity connected with the calorimeter structure. Note that the same behaviour of response distribution was observed experimentally by the SPACAL collaboration [4].

To study the SciFi calorimeter response variation due to structure inhomogeneity we carried out a set of calorimeter response simulations for different fixed impact points at three incident energies 5, 40, and 120 GeV. At each incident energy 100 different impact points were randomly generated with a uniform distribution in an 1×1 cm^2 area around the module centre. At each impact point 1000 events were simulated for the energy 5 GeV and 500 events for the energies 40 and 120 GeV. This approach provided us with the local response distributions (corresponding to fixed impact points) and local energy resolutions for each of the 100 impact points. The simulation was carried out for the passive-active material ratio 4:1, fibre radius 1mm and tilt angle 3°.

The results of the simulation are presented in Tables 1,2 and Figures 5—7. Table 1 summarizes the basic results obtained for three incident energies ($E_{inc} = 5$, 40, and 120 GeV). For each energy Table 1 contains the average local response of the SciFi calorimeter ($\overline{E}$), the standard deviation (caused by nonuniformity) of the average local response distribution (σ_{non}), the average standard deviation (caused by sampling fluctuations) for local response distributions (σ_0), the energy resolution calculated as $\sqrt{(\sigma_{non}^2 + \sigma_0^2)}/\overline{E}$, and the energy resolution for the wide beam (ε_{wb}). For comparison, in Table 1 we also present the values of the systematic term calculated on the basis of a theoretical model presented below (see (9) and comments therein). The comparison of the calorimeter global energy

Table 1. Influence of the SciFi calorimeter structure inhomogeneity on the calorimeter energy resolution (the simulation results). E_{inc} is the incident energy, $\overline{E}$ is the average local response of the SciFi calorimeter; σ_{non} is the standard deviation (caused by nonuniformity) of the average local response distribution; σ_{non}^{th} is the standard deviation calculated on the basis of the second term in (9); σ_0 is the average standard deviation (caused by sampling fluctuations) for the local response distributions; ε_{wb} is the energy resolution for the wide beam

E_{inc}	[GeV]	5	40	120
$\overline{E}$	[MeV]	116.7 ± 0.4	936.2 ± 2.7	2812 ± 8
σ_{non}	[MeV]	4.5 ± 0.3	27.2 ± 1.3	80 ± 6
σ_{non}^{th}	[MeV]	5.3 ± 0.2	30.6 ± 0.8	80.40 ± 2.10
σ_0	[MeV]	8.18 ± 0.07	25.3 ± 0.2	47.9 ± 0.5
$\sqrt{(\sigma_{non}^2+\sigma_0^2)}/\overline{E}$	[%]	8.0 ± 0.5	4.0 ± 0.3	3.3 ± 0.2
ε_{wb}	[%]	8.12 ± 0.20	4.58 ± 0.20	3.14 ± 0.10

Table 2. Average response and energy resolution for the wide beam (global) and for the beam with the fixed impact point (local), obtained by MC simulation

	Average response [MeV]		Energy resolution (%)	
E_{inc} [GeV]	local	global	local	global
1	24.32	23.31	13.19±0.21	15.28±0.24
2	44.88	46.45	10.57±0.24	11.32±0.25
5	115.12	113.75	6.97±0.11	8.12±0.20
10	232.71	232.91	5.14±0.08	6.10±0.10
20	471.71	467.38	3.76±0.08	4.80±0.11
40	936.05	933.28	2.65±0.06	4.04±0.09
80	—	1862.18	—	3.42±0.08
120	2878.61	2798.07	1.53±0.03	3.14±0.10
200	4813.00	4661.55	1.17±0.04	2.89±0.06

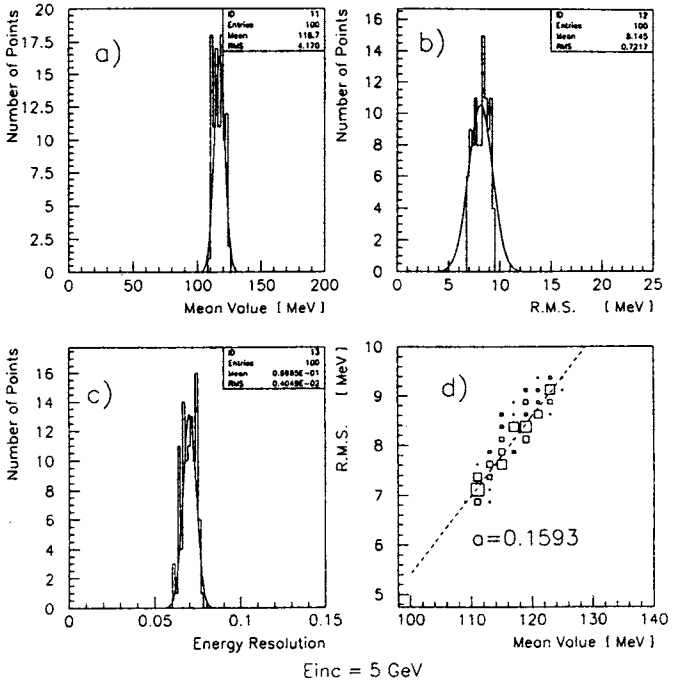

Fig.5. Local response simulation results for 5 GeV incident particles and the fixed impact points scattered over the 1 × 1 cm^2 area; distribution of: a) local average responses; b) R.M.S. of local response distributions; c) local energy resolutions; d) local R.M.S. vs. local average response

resolution determined by the method of wide beam simulation (ε_{wb}) and that determined on the basis of the local response distribution characteristics (σ_0, σ_{non}) leads to good agreement between these two approaches. In Table 2 the responses and resolutions, obtained by MC simulation, are shown for the wide beam and the beam with a fixed incident point for a set of incident energies (1—200 GeV). The fixed point in the latter case was chosen as the point with the average local response equal to the average global one at the incident energy 10 GeV.

In Fig.5a the distribution of the average local responses for the incident energy 5 GeV is presented. The distribution of the local standard deviations is given in Fig.5b and that of the local resolutions is depicted in Fig.5c. In Fig.5d the dependence of the local standard deviation on the average local response is presented as a two-dimensional «box» plot, where the box size is proportional to the number of cases. From Fig.5d one can see that the standard deviation of the local response (σ_i) has a tendency to grow approximately linearly with the average local response $\overline{E}_i$, which is in good agreement with (7). Fitting the

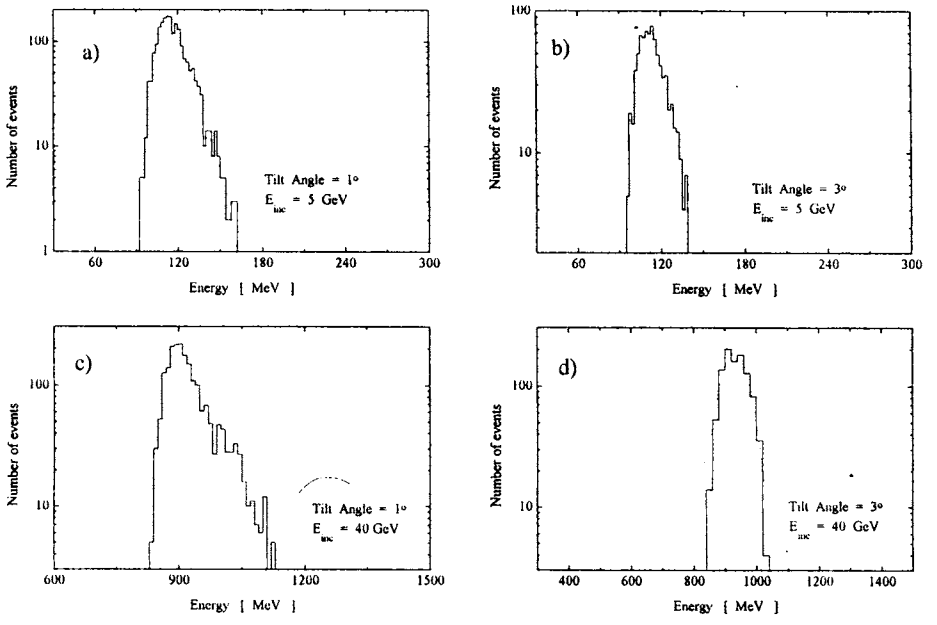

Fig.6. SciFi calorimeter response for 5 and 40 GeV incident particles at two different tilt angles (1° and 3°)

histograms in Fig.5d, as well as the analogous histograms for 40 and 120 GeV, by means of (7) we obtained $\Delta \approx 0.16$ for 5 GeV, $\Delta \approx 0.05$ for 40 GeV and $\Delta \approx 0.036$ for 120 GeV. The nonzero Δ measures the deviation of the global response shape from the Gaussian form. From the fitted values of Δ we see that the distortion decreases with increasing incident energy. In the case of the SciFi calorimeter the distortion could be especially large for high passive-to-active material ratios ($\geq 4:1$), small tilt angles ($\leq 3°$), and large fibre diameters (≥ 1 mm). The above-mentioned effect is demonstrated in Figs.6a-d, where the simulated global responses for two incident energies 5 and 40 GeV and two tilt angles: 1° and 3° are shown. From Figs.6a and 6c, where the responses for the incident energy 5 GeV and 40 GeV and tilt angle 1° are presented, it is obvious that the response distribution has a Gaussian-like shape with an enhanced right tail. The distortion of the Gaussian shape of the response at higher energies and higher tilt angles (Figs.6b-d) is not so impressive and hence we can conclude that the distortion decreases with increasing tilt angle and increasing incident energy. For these conditions the response tends to a Gaussian form with the standard deviation $\sigma = \sqrt{\sigma_0^2 + \sigma_{non}^2}$. The fact that σ is a quadratic sum of σ_0 (sampling fluctuations) and σ_{non} (response nonuniformity) confirms correctness of using formula (1) for energy resolution parametrization.

The presented results stress the significant role of the calorimeter structure inhomogeneity. The ratio $\sigma_{non}/\overline{E}$, i.e., the nonuniformity contribution to the energy resolution, is

$3.8 \pm 0.2\%$ at 5 GeV, $2.9 \pm 0.2\%$ at 40 GeV, and $2.8 \pm 0.2\%$ at 120 GeV. Consequently, this ratio exhibits only weak dependence on the incident energy and thereby will effectively influence only the constant term. This fact makes us conclude that the structure inhomogeneity contributes to the constant term b if the energy resolution is parametrized by means of formula (1). Using this formula to fit the dependencies in Table 2 for the wide and narrow beams we obtained the following values of the parameters: $a = 15.91 \pm 0.17$ and $b = 2.89 \pm 0.05$ (wide beam) and $a = 15.90 \pm 0.14$ and $b = 0.43 \pm 0.07$ (narrow beam). In both cases χ^2 are bad, 6.34 and 3.35, respectively. The bad χ^2 suggests that the weak energy dependence of the $\sigma_{non}/\overline{E}$ ratio plays a role in this case. To unravel the problem we looked at this dependence more carefully. The main issue is that the size of the electromagnetic shower increases with incident energy, which makes the elements of the calorimeter structure relatively smaller as compared with the effective size of the shower. In general, it means that the inhomogeneities will be less important if the incident energy increases. To estimate the dependence of $\sigma_{non}/\overline{E}$ on energy we define the effective volume of the shower as

$$V = \text{const} \, (\ln (E/E_{thr}))^3, \tag{8}$$

where E is the incident energy and E_{thr} is the threshold energy, which can be chosen as the energy at which an electromagnetic shower starts, i.e., the energy of pair production (1 MeV). Assuming that the response fluctuations connected with inhomogeneities ($\sigma_{non}/\overline{E}$) are proportional to $1/\sqrt{V}$, which corresponds to the Poissonic nature of the fluctuations, we can parametrize the energy resolution as

$$\frac{\sigma}{E} = \frac{a}{\sqrt{E}} \oplus \frac{\tilde{b}}{\left(\ln \frac{E}{E_{thr}} \right)^{3/2}}. \tag{9}$$

For better understanding of the assumption $\sigma_{non} \sim \sqrt{V}$ used in (9) some qualitative arguments can be given. The number of the active calorimeter elements involved in the shower (n_{eff}) is proportional to the effective shower volume V and it is natural to suppose that n_{eff} obeys the Poisson law, which immediately leads to $\sigma_{non} \sim \sqrt{V}$.

It should also be noted that the choice of E_{thr} as the pair production energy is, to some extent, arbitrary and other choices could be taken, e.g., the critical energy can be taken as E_{thr}. Also, the second term in (9), reflecting the calorimeter inhomogeneity, is only one of possible parametrizations of the inhomogeneity term which are based on the idea that the manifestation of inhomogeneity will diminish as a function of the incident energy logarithm.

In Fig.7, the energy resolution is presented as a function of the energy for a wide (1×1 cm^2) beam and for the beam with a fixed impact point fitted by two different parametrization formulae (9) and (1). In Fig.7a the simulated data for the wide beam were fitted

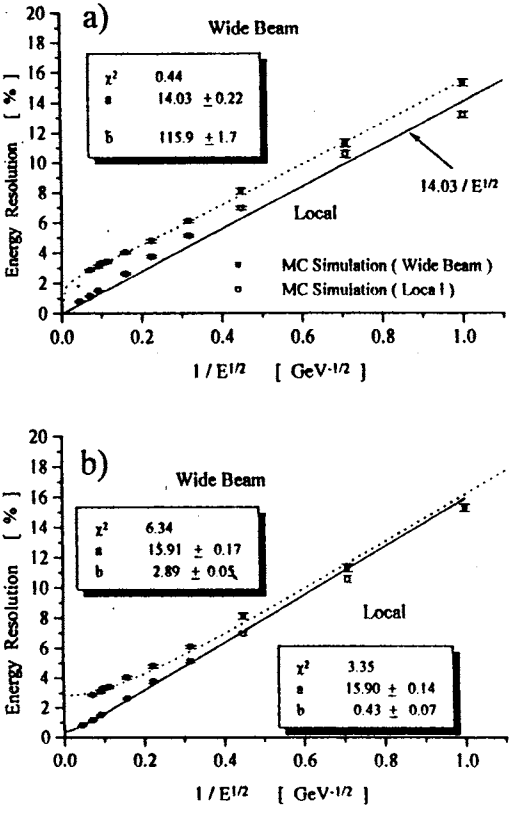

Fig.7. a) Energy resolution for the wide beam (solid squares) fitted by (9) (dashed line) and local energy resolution for one fixed impact point (open squares, full line). b) Energy resolution for the wide beam fitted by (1) (dashed line) and local energy resolution for one fixed impact point

using formula (9). The fit was good with $\chi^2 = 0.44$ and parameters $a = 14.03 \pm 0.22$ and $\tilde{b} = 115.9 \pm 1.7$. The inhomogeneity term should not be present in the fixed impact point data, but superimposing these data on the sampling term line $(14.03/\sqrt{E})$ we can see that the data are slightly scattered around the line.

We note that the fixed impact point was chosen as the point with the average local response equal to the average global one at the incident energy 10 GeV. The fact that the fixed impact point data are «scattered» can be explained if we realise that at the incident energy different from 10 GeV the average local response can be shifted against the global one. It means that at energy other than 10 GeV the sampling fraction for the chosen fixed point is not equal to the mean sampling fraction at this incident energy. The latter statement is well demonstrated in Table 2, where the data concerning the local and global data are compared. Hence, one can conclude that in the case of a fixed impact point the constant term is consistent with zero in the error limits. The inhomogeneity term in formula (9) is also in good agreement with the calorimeter inhomogeneity data mentioned above $(\sigma_{non}/\overline{E})$, as can be seen from Table 1 comparing σ_{non} and σ_{non}^{th}. Agreement is very good at 40 and 120 GeV and a slight overestimation is seen at 5 GeV. It is remarkable that two different approaches, one based on the wide beam resolution, and the other based on the average local responses, comply with each other. This fact makes the inhomogeneity term parametrization to be proper.

Note that the second term in formula (9) tends to zero if the incident energy goes to infinity, hence the fluctuations connected with inhomogeneity vanish as $E \to \infty$. On the other hand, for the energies below 1 TeV the constant term effectively exists for the wide-spot beam and its value is about 2.9%,which is the result of the fit with function (1) – see Fig.7b. Moreover, in a real case there are also other sources of fluctuations as the fluctuations corresponding to energy leakage, light attenuation in fibres, etc. The former ones, if compared with the fluctuations originated in inhomogeneity, have just opposite tendency

of behaviour with the increasing incident energy. Therefore one can expect that in real cases the constant term is present. Formula (9) should be treated as a formula for an idealised case, where only sampling fluctuations and those connected with structural inhomogeneities are present.

4. Summary and Conclusions

The mode of operation of SciFi calorimeters, where particles enter at small tilt angles in respect to the direction of the fibers, makes them feel the inhomogeneous structure of the calorimeter. Due to narrowness of electromagnetic showers at the initial stage, the effect of inhomogeneity is not completely averaged after the shower completion and manifests itself as dependence of the calorimeter mean signal on the impact point position on the calorimeter surface. The effect is more pronounced for:

- small tilt angles;
- high absorber-to-fiber volume ratios;
- small incident energies.

This effect has visible consequences at the interpretation of the results from the SciFi calorimeter modules tested in beams which obviously have the transverse spread greater than the fiber-to-fiber distance.

In this paper it is shown on the basis of Monte-Carlo simulation that:

1. The calorimeter response distribution is additionally broadened due to dependence of the calorimeter mean response on the position of the impact point. This is the main source of the systematic term in the energy resolution parametrization formula. In our treatment it is demonstrated on the basis of general statistical arguments that the two terms (stochastic and systematic) in the parametrization formula must be added quadratically. In the literature one can often find a formula where they are added linearly.

2. The calorimeter signal for the case with the beam spot greater than the fiber-to-fiber distance is no more Gaussian distributed. In addition, its distribution exhibits an asymmetry with a tail towards the high-energy part.

3. Both the asymmetry and the systematic term have a tendency to decrease slowly with the incident energy. Based on intuitive arguments, parametrizations of this dependence for the asymmetry and the systematic term were found.

Appendix A

Analytical expression for the calorimeter global response. Assuming that the average local response $\overline{E}_i$ has Gaussian distribution with the average $\overline{E}$ and the standard deviation σ_{non}, we can replace the summation in expression (2) by integration:

$$w_{gl}(E) \simeq \frac{1}{\sqrt{2\pi}\sigma_{non}} \int d\bar{E}_i \exp\left(-\frac{(\bar{E}_i - \bar{E})^2}{2\sigma_{non}^2}\right) \frac{1}{\sqrt{2\pi}\sigma_i} \exp\left(-\frac{(E-\bar{E}_i)^2}{2\sigma_i^2}\right). \qquad (A.1)$$

Using (7) for σ_i and the Taylor expansion in the parameter of the second exponent under integral (A.1) we obtain

$$w_{gl}(E) = \frac{\exp\left(\frac{(E-\bar{E})}{2\sigma_T^2}\right)}{\sqrt{2\pi}\sigma_T}\left[1 + \Delta \cdot f_1\left(\frac{E-\bar{E}}{\sigma_T}\right) + \frac{\Delta^2}{2} f_2\left(\frac{E-\bar{E}}{\sigma_T}\right) + \ldots\right], \qquad (A.2)$$

where $\sigma_T = \sqrt{\sigma_0^2 + \sigma_{non}^2}$ is the full standard deviation when the asymmetry is not present ($\Delta = 0$) and the functions $f_i(\varepsilon)$ can be expressed analytically. For simplicity, we give only the function $f_1(\varepsilon)$:

$$f_1(\varepsilon) = \frac{\sigma_0^2 \cdot \sigma_{non}}{\sigma_T^3}(\varepsilon^3 - 3\varepsilon). \qquad (A.3)$$

The fact that $f_1(\varepsilon)$ is antisymmetric, positive for $\varepsilon > \sqrt{3}$ and negative for $\varepsilon < -\sqrt{3}$ brings about the asymmetry of the global distribution ($w_{gl}(E)$) with an enhanced right tail. We note that $f_2(\varepsilon)$ is symmetric ($f_2(\varepsilon) = c_0 + c_1\varepsilon^2 + c_2\varepsilon^4 + c_3\varepsilon^6$, where c_i are polynomials of σ_0/σ_T) and therefore does not contribute to the asymmetry but only increases the width of the global distribution.

Acknowledgements

The authors thank Jozef Masarik for useful advice and help during the preparation of this paper.

References

1. Wigmans R. — Proc. of the 2nd Int. Conf. on Calorimetry in High Energy Physics, Capri, Italy 14—18 October, 1991, edit. A.Ereditato, World Scientific, 1992, p.24.
2. Acosta D. et al. — Nucl. Instr. and Meth., 1991, v.A308, p.481.
3. Gringrich D.M. et al. — Nucl. Instr. and Meth., 1995, v.A364, p.290.
4. Livan M., Vercesi V., Wigmans R. — Scintillating Fibre Calorimetry, CERN 95-02 (1995) and references therein.
5. Fabjan C. — Experimental Techniques in High Energy Physics, edited by T.Ferkel, Addison Wesley, 1997.

6. Budagov J. et al. — Nucl. Instr. and Meth., 1994, v.A343, p.476.
7. Štavina P. et al. — Nucl. Instr. and Meth., 1995, v.A364, p.124.
8. Budagov J. et al. — Nucl. Instr. and Meth., 1995, v.A362, p.395.
9. Vercesi V. — Large Hadron Collider Workshop, CERN 90-10, vol. III, p.14.
10. Brun R. et al. — GEANT — CERN Program Library, W5013.

Received on March 3, 1998.